Assignments of Normally Unoccupied Orbitals to the Temporary Negative Ion States of Several Lanthanide NMR Shift Reagents and Comments on Resonance Involvement in Electron Circular Dichroism

A. M. Scheer, G. A. Gallup, and T. J. Gay*

Behlen Laboratory of Physics, University of Nebraska, Lincoln, Nebraska 68588-0111

Received: December 6, 2007; In Final Form: February 7, 2008

We have measured the total electron scattering cross sections of several NMR shift reagent molecules $X(hfc)_3$, where X = Yb, Er, Eu and Pr, by means of electron transmission spectroscopy (ETS) to determine their vertical attachment energies. A strong low-energy resonance (<1 eV) is observed in all of the compounds except for $Yb(hfc)_3$. We explain this anomaly in terms of the ground-state electron configuration of each molecule. Also, with the aid of restricted open-shell Hartree−Fock (ROHF) calculations on analogous molecules with truncated fluorocarbon chains, we have assigned specific normally unoccupied orbitals to the resonances observed in ETS. To our knowledge, these molecules are the largest for which this procedure has been successfully completed. Nolting et al. (*J. Phys. B* **1997**, *30*, 5491) have demonstrated that the above NMR shift reagents exhibit electron circular dichroism (ECD) between 1 and 10 eV. Using our new total cross section data, we comment on the possibility of resonance involvement in the generation of ECD.

Introduction

As understanding of gas-phase temporary negative ions (TNIs) generated by electron impact has progressed, the need to examine large molecules has become increasingly important.[1] A major challenge in studies involving TNIs of large molecules is the assignment of resonances in the total electron scattering cross sections to specific virtual orbitals (VOs) predicted by quantum chemical calculations. In this work, we report new electron transmission spectroscopy (ETS)[2] measurements on the four NMR shift reagent compounds X tris[3-(heptafluoropropylhydroxylmethylene)-(+/-)-camphorate], $X(hfc)_3$, where *X* = Yb, Er, Eu and Pr. These spectra extend the energy range to lower values than had been previously reported,[3,4] allowing the observation of new features below 1 eV.

With atomic weights of greater than 1200, we believe this study represents the largest systems for which normally unoccupied orbitals have been assigned. To assign specific normally unoccupied orbitals to resonances observed in ETS, we have performed restricted open-shell Hartree−Fock (ROHF) calculations on $Yb(tfc)_3$ and $Pr(tfc)_3$ where the "t" indicates that the $CF_2CF_2CF_3$ fluorocarbon chains have been replaced by CF_3 groups to simplify the computations. We do not expect this to inhibit comparison to the experimental spectra for two reasons. First, resonances of Σ character centered on second-row atoms are broad, overlap one another, and exist at high energies.[5] Resonances of Π character are characteristically strong and often will further obscure resonances resulting from direct injection into pure σ^* orbitals. As will be detailed later, the NMR shift reagents studied in this work all contain local resonances of local π^* character. For these reasons, σ^* resonances are not expected to be discernible here. Second, the six-membered, quasi-aromatic ring structures of these molecules that give rise to the strong resonances seen in our transmission spectra are a large distance from the fluorocarbon chains. Thus wave functions associated with these moieties are largely decoupled from the central regions and truncation should not significantly affect the relevant orbitals, or the trends in VO energies (VOEs).

Another motivation of this work has been to investigate the correlation between the total electron scattering cross section resonances of these compounds and features in electron circular dichroism (ECD). Electron circular dichroism is the preferential scattering of spin-polarized electrons by chiral molecules, in analogy with optical circular dichroism and will be discussed further below. By comparing the positions and trends of resonances in the total scattering cross section with features in ECD spectra reported by the Münster group,[4] we can comment on the possibility of resonance involvement in the generation of ECD.

Electron Transmission Spectra

Low-energy scattering resonances can arise when an electron becomes transiently bound in a normally unoccupied molecular orbital, thus forming a temporary negative ion (TNI). To determine the vertical attachment energies (VAEs), i.e., resonance energies of the NMR shift reagents, we have examined their TNI states using electron transmission spectroscopy (ETS).[2] The Münster group has previously reported the ET spectrum for $Yb(hfc)_3$ [3] and less specific resonance energy regions for the remaining shift reagents (Figure 2 of ref 4).

In our experiment, a magnetically collimated, monoenergetic electron beam is transmitted through a collision cell containing a target vapor. Scattered electrons are rejected by a retarding electrode following the collision cell and the transmitted electrons are collected. For a given incident electron energy and energy loss, the retarding voltage determines the range of electron scattering angles that are rejected. To accentuate resonant structure in the cross section, a small modulation voltage is applied directly to the collision cell and the AC component of the transmitted current is detected by a lock-in amplifier, enabling determination of the derivative of transmitted

* Corresponding author. E-mail: tgay1@unl.edu.

10.1021/jp7115164 CCC: $40.75
Published on Web 03/28/2008

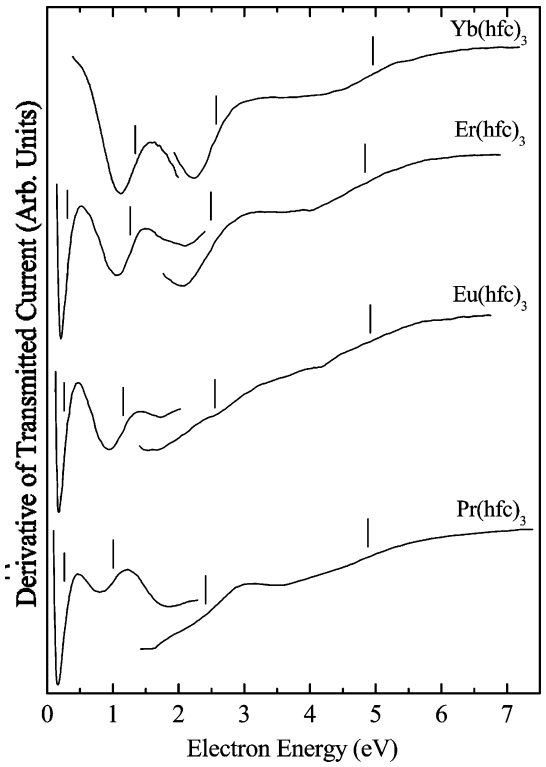

Figure 1. Derivative with respect to electron energy of current transmitted through gas-phase $Yb(hfc)_3$, $Er(hfc)_3$, $Eu(hfc)_3$, and $Pr(hfc)_3$. Vertical attachment energies (VAEs) are indicated by short vertical bars.

current with respect to energy. In the derivative signal, a peak in the total scattering cross section is thus indicated by a minimum followed by a maximum. The resonance energy is assigned to the *vertical* midpoint of this dip-to-peak structure. Because the electron attachment process is rapid relative to nuclear motion, the resonance energy characterizes the molecule in its neutral equilibrium geometry and is a measure of the VAE. A peak at 2.46 eV in the derivative signal of N_2 associated with vibrational structure ($\nu = 2$) of the $^2\Pi_g$ anion state is used to provide an energy calibration of the ET spectra, as was done in ref 6. A trochoidal electron monochromator[7] provided an incident electron energy width between 40 and 80 meV. The absolute uncertainty in the determination of resonance energies is ± 0.05 eV.

At room temperature the NMR shift reagents in question have very low vapor pressure. They were introduced into the collision cell by means of a sample oven directly attached to the collision chamber. The oven and collision cell were separately heated with the cell kept slightly warmer to avoid condensation. To obtain adequate vapor pressure, the sample oven temperatures required were 117 and 132 C for $Er(hfc)_3$ and $Eu(hfc)_3$ respectively. We were unable to obtain temperature measurements in the $Pr(hfc)_3$ and $Yb(hfc)_3$ experiments due to inadvertent detachment of the thermocouple leads. In the case of $Yb(hfc)_3$, slightly more current through the sample oven and collision cell heater was required than was necessary for the other compounds, indicating a higher temperature. Measurements were taken with 10−40% attenuation of the electron beam. The ET profiles remained unchanged with increasing temperature, indicating that no significant sample decomposition leading to gaseous impurities was occurring.

In Figure 1 we present the ET spectra for the compounds studied here, plotting the derivative of the transmitted current as a function of incident electron energy. Vertical lines indicate the midpoints of the resonances. Weaker retarding voltages are employed at higher energies to avoid variations in the transmitted current due to misalignment of the magnetic field with the electron beam.[8] The breaks in the curves separate spectra obtained with different retarding voltages and different scaling factors. The curves are overlapped to show energy agreement. It is possible that small changes in the width of the dip-to-peak structure characteristic of a resonance exist between the low- and high-energy spectra due to the different retarding voltages. We do not expect that this will significantly alter the position of the vertical midpoint of the resonances.

TABLE 1: Vertical Attachment Energies (VAEs) from the Münster Lab[3] for $Yb(hfc)_3$ and from This Work for $X(hfc)_3$, with X Being Yb, Er, Eu and Pr[a]

	VAE	VAE	ECD	VAE	ECD	VAE	ECD
$Yb(hfc)_3$[3]		1.7		2.8		6.0	
$Yb(hfc)_3$		1.3	1.6	2.6	2.5	5.0	5.6
$Er(hfc)_3$	0.3	1.3	1.7	2.5	2.4	4.8	5.4
$Eu(hfc)_3$	0.3	1.2	1.3	2.6	1.9	4.9	5.0
$Pr(hfc)_3$	0.3	1.1	U	2.4	1.9	4.9	4.7

[a] The maxima and minima observed in asymmetry (ECD)[3] that would be assigned to these resonances based on the $Yb(hfc)_3$ data (see text) are also indicated. The "U" indicates an unobserved feature. All energies are in eV.

A strong low-energy resonance is observed in each of the compounds except $Yb(hfc)_3$. We will explain this anomaly below. Each spectrum shows two strong resonances between 1 and 3 eV and a broad higher energy resonance near 5 eV. Table 1 gives the VAEs for all of the reagents, along with the resonance energies reported by the Münster group[3] for $Yb(hfc)_3$.

The ET spectrum of $Yb(hfc)_3$ given in ref 3 and the resonance positions reported in ref 4 for the remaining compounds were obtained with a technique similar to ours. The two ET spectra of $Yb(hfc)_3$ agree qualitatively. However, as indicated in Table 1 for $Yb(hfc)_3$, the vertical midpoints of the resonances observed in ref 3 are seen at somewhat higher energies. These discrepancies arise, at least in part, because we use a retarding voltage to greatly restrict the forward scattering acceptance angle, thus providing a measurement as close as possible to the total scattering cross section. Mayer et al.[3] do not use this procedure and thus measure cross sections less restricted to forward scattering. Therefore, when we compare our spectra with those of the Münster group, shifts in resonance energies are not surprising. We expect that the shifts seen in the case of $Yb(hfc)_3$ exist for the other reagents as well. Further details of the effects of the retarding voltage on ET spectra can be found in ref 8.

Theory

The molecules considered in this article are members of a large group of compounds of transition metals, lanthanides, and actinides with organic ligands. When the ligand is bidentate, i.e., when it contains two attaching groups, those metals that bind ligands octahedrally will form compounds that have three ligands arranged in two possible "propeller" configurations. In the fixed nucleus approximation (FNA), nuclear positions and the electronic wave function satisfy D_3 symmetry, a group with no improper elements. If the two ligand attachment points are equivalent, these two enantiomers are the only possibilities. In contrast, we are dealing with a modified camphor ligand that has both intrinsic chirality and nonequivalent attachment points. Ignoring the chirality, the nonequivalence of the attachment points provides eight possible enantiomers. If we arbitrarily refer

TABLE 2: C_3 Character Table

C_3	E	C_3	C_3^2
A	1	1	1
E_1	1	ϵ^a	ϵ^*
E_2	1	ϵ^*	ϵ

[a] $\epsilon = \exp(2\pi i/3)$.

to the two orientations of the camphor molecules as U (up) or D (down), we have U_3, U_2D, UD_2, and D_3, with the two mixed cases having 3 times the statistical weight of the other two. Of these, only U_3 and D_3 satisfy any symmetry operations; they belong to the C_3 group.

For reference, we give the C_3 character table in Table 2. This group has complex one-dimensional characters, but the energies are either nondegenerate and of species A or doubly degerate and of species $\{E_1\ E_2\}$. The four metals we are concerned with all have 4f electrons, and in the compound they are subject to a C_3 ligand field.[9] Standard methods allow us to determine that the spherical {4f} set is no longer 7-fold degenerate in energy but is split into five different energies with symmetry types {a a a e e} in the lower symmetry environment. This is not necessarily the order of the new energies.

We have carried out restricted open-shell Hartree−Fock (ROHF) calculations on the Pr and Yb compounds, slightly simplified, but very closely related to the corresponding shift reagent molecules actually studied in the laboratory. The latter have ligands possessing a heptafluorocarbon chain, attached at one point and, as in the introduction, are referred to generically with symbol $X(hfc)_3$. As previously discussed, the location and nature of such a fluorocarbon chain strongly suggests that truncating this to the simpler $-CF_3$ group will have no substantial effect upon the results from these calculations. In the succeeding arguments we distinguish the calculated molecules from the measured ones by labeling the former as $Pr(tfc)_3$ and $Yb(tfc)_3$. The Pr and Yb compounds were chosen for calculation because they have nearly empty and nearly full f-shells on the central metal atom, respectively. The $Er(tfc)_3$ and $Eu(tfc)_3$ molecules are expected to be almost intractable within the ROHF procedure.

The GAMESS[10] program was employed for the calculations using its built-in "MINI" basis set.[11] Some modules from the CRUNCH suite[12,13] were also required. The Molekel 3D plotting software[14] was used to render the orbital drawings illustrated below. Using $Yb(tfc)_3$ as an example, the following is an outline of the computational procedure used. The geometry of the skeleton for one of the C_3 propeller versions of the $Yb(tfc)_3$ is shown in Figure 2. In $Yb(tfc)_3$, the Yb is in a (III) oxidation state, resulting in the compound having a multiplicity of two. The electron configuration of neutral Yb is $[Xe]:(4f)^{14}(6s),^2$ and when it loses three electrons to form the compound, the configuration becomes $[Xe]:(4f).^{13}$ Our calculations indicate no tendency for the compound to involve the Xe core.

If the Yb^{+3} ion were isolated and satisfied L−S coupling rules it would have $L = 3$ and $S = {}^1/_2$. However, the symmetry of the molecule is trigonal, and as discussed above, there are three ^2A and two ^2E states possible from the single f-hole (see tables in ref 15). These have somewhat different energies and can be expected to cause significant problems with convergence during ROHF calculations. In addition, a complicated Roothaan-type state averaging procedure would be required to separate the lowest A- or E-state energies if they were required.

An individual isolated ligand molecule can be in two different atomic arrangements, the enol or keto forms. These are shown in Figures 3 and 4, respectively. It is the less stable enol form

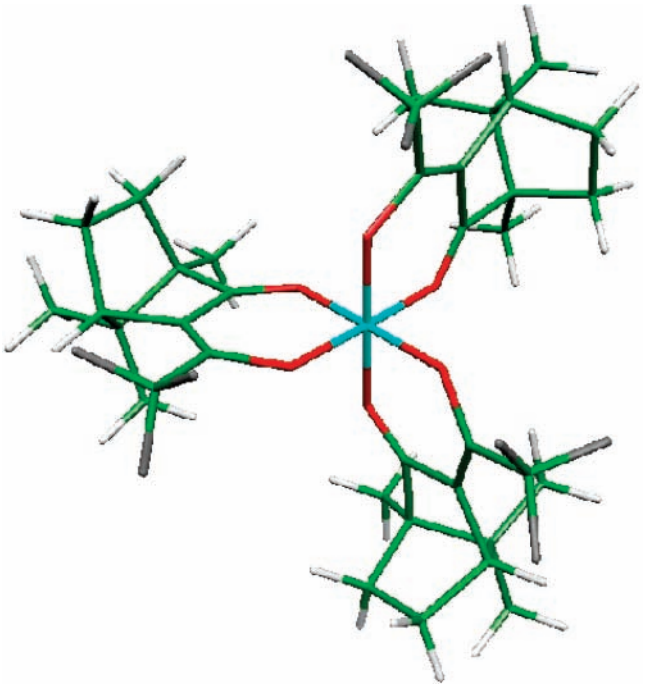

Figure 2. Framework structure of $Yb(tfc)_3$. The green rods represent carbon bonds. Hydrogen bonds are represented by white, oxygen by red, fluorine by gray, and ytterbium by light blue.

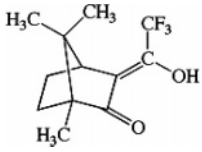

Figure 3. Enol structure that bonds to Yb after losing a H^+ attached to the enol O atom.

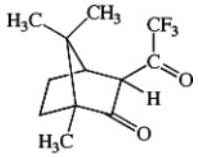

Figure 4. Keto structure, in its most stable native form.

that loses the H^+ to produce the negatively charged ligand. There is a C═C double bond in each of the three ligands in addition to the C═O double bond, and they are conjugated. This means that the O═C−C═C−O− part of the ligand is planar, and the coordination compound has three equivalent, nearly planar six-membered rings when the Yb is counted, as can be seen in Figure 2. Our calculations of the lowest energy {e} set (Figure 5) and the next higher energy {e} set (Figure 6) indicate that the precise bonding pattern in the enol structure does not carry over to the molecule. Rather, the form of the ligand in the coordination compound is a resonance hybrid of the bond structure of the enol and keto tautomers:

$$Yb_{1/6}-O{=}C-C{=}C-O-Yb_{1/6} \leftrightarrow Yb_{1/6}-O-C{=}C-C{=}O-Yb_{1/6}$$

Earlier, we pointed out that there are eight propeller conformers possible in any of these compounds. The calculations were restricted, however, to the D_3 (or U_3) enantiomers. (We may note that this symmetry greatly improves the chances that the ROHF procedure will converge.) Although these are in the minority statistically, the inner structure of the compounds with

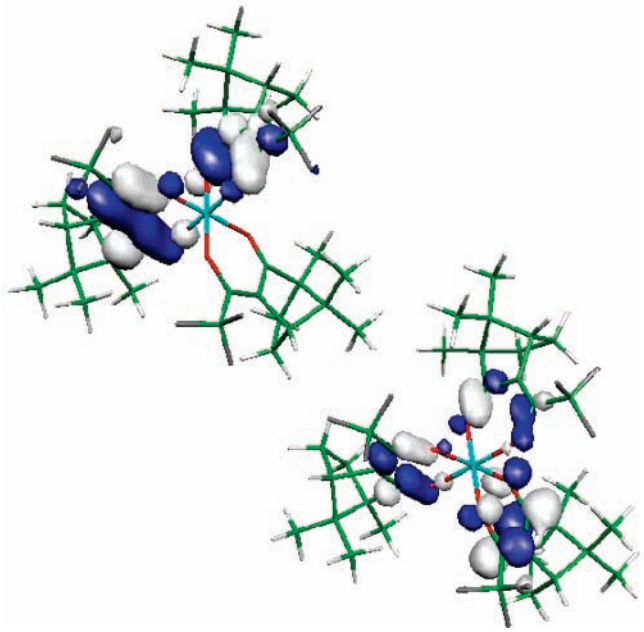

Figure 5. First {e} set among the virtual orbitals. This involves mainly locally π-like orbitals on the ligand−Yb rings.

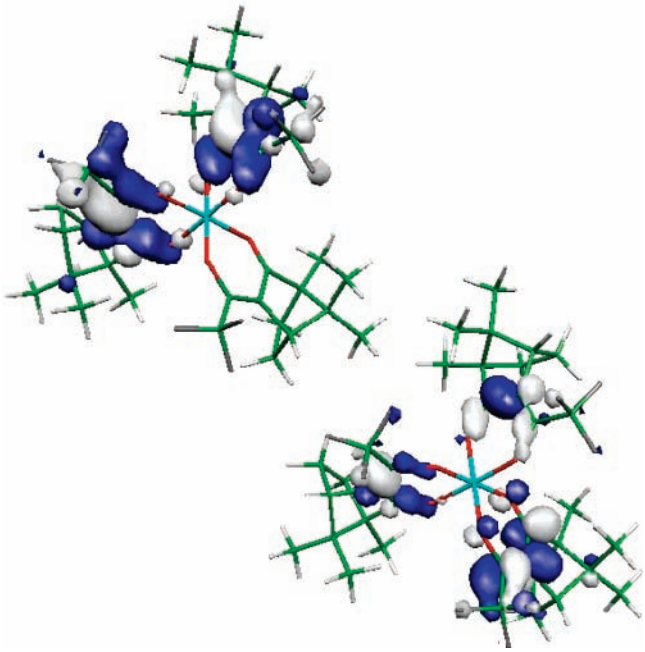

Figure 6. Second {e} set among the virtual orbitals. These also mainly involve locally π-like orbitals on the ligand−Yb rings.

their three six-membered ring arrangement is necessarily very much the same in all of the isomers, and calculations confirm that virtual orbitals (VOs) producing resonances are largely confined to this inner region.

It has been shown from ETS measurements that ground state shape resonances of molecules can be associated with VOs of Hartree−Fock (HF) calculations,[16] particularly when the orbital involved has a leading l-wave with $l = 1$ or higher. The {e} type orbitals of C_3 symmetry have this characteristic, and in Figures 5−7 we show these from our calculation of the Yb(tfc)$_3$ molecule. In the two lower energy {e} orbitals there is considerable local-π character, and this will tend to increase the average value of l in the composite l-wave, decrease its energy width, and thus make it more prominent in ETS. It is also interesting to consider the singly occupied molecular orbital

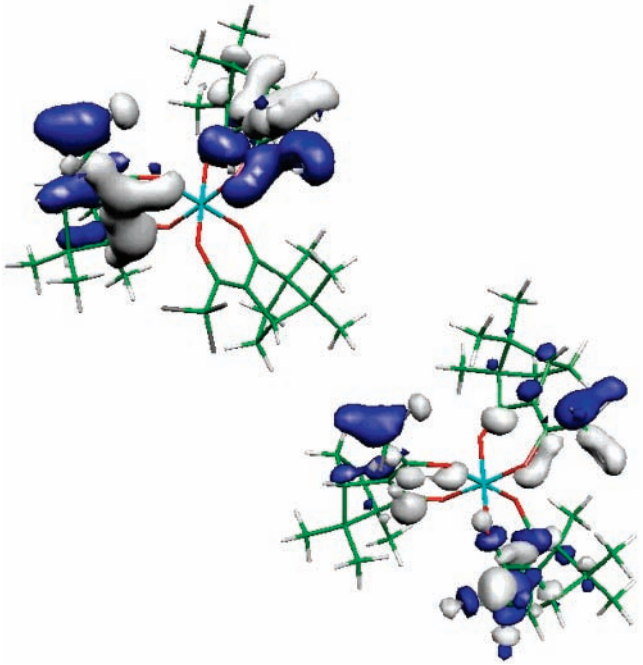

Figure 7. Third {e} set among the virtual orbitals. These involve antibonding orbitals from the CF_3 groups and from C−H bonds.

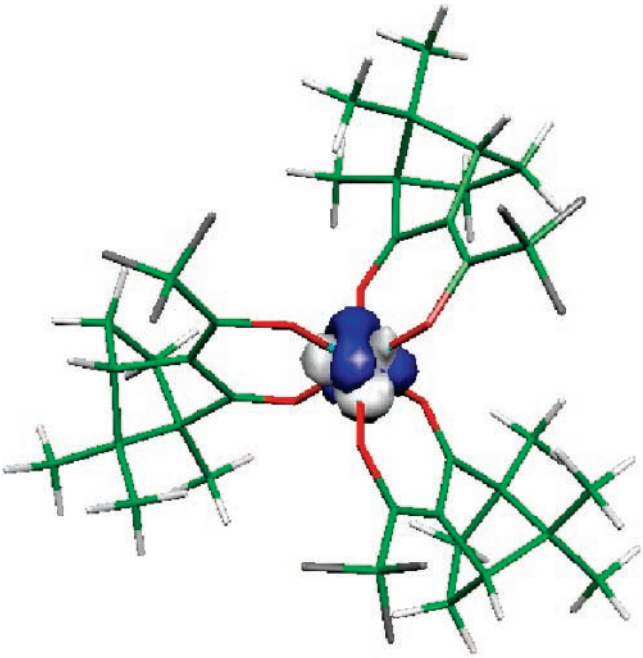

Figure 8. SOMO of Yb(tfc)$_3$. It is essentially an f_{xyz} orbital and the hole is the same.

(SOMO), and we show in Figure 8 that it is entirely on the Yb atom at the default value of the absolute orbital amplitude of the plotted iso-surface (0.05 $a_0^{-3/2}$).

The true VOs of type {e} present in Pr(tfc)$_3$ are essentially indistinguishable from those in Yb(tfc)$_3$. The difference arises with the SOMOs in Pr(tfc)$_3$. Because all but one of the f-orbitals in Yb(tfc)$_3$ are occupied, essentially only one a-type orbital remains. On the other hand, Pr(tfc)$_3$ has only two f-electrons to contribute to the molecule, and following Hund's rule, they occupy two different {e}-type orbitals singly in an overall ^{3}A state.[15] We show these in Figure 9. Thus Pr(tfc)$_3$ has two empty {e}-type spin orbitals, the complements of those singly occupied in the ^{3}A state, and they can support an {e}-type resonance with a lowest l not less than one. The results of the calculations are

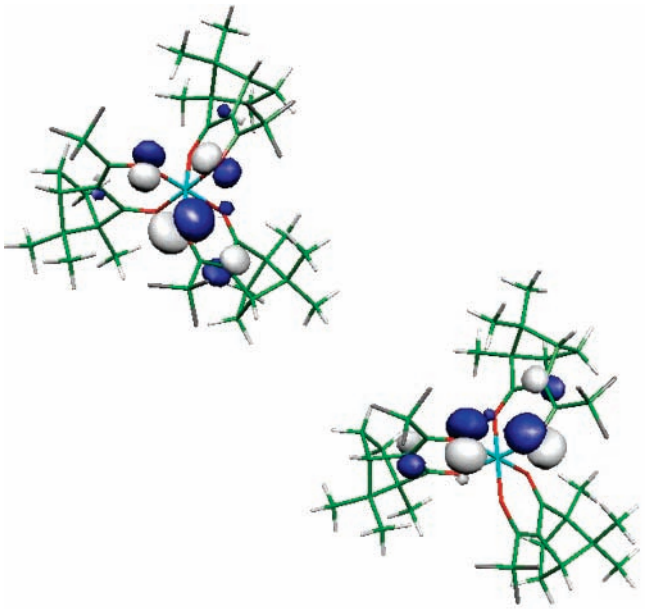

Figure 9. SOMOs of $Pr(tfc)_3$ showing the e_1 and e_2 orbitals that are coupled to the ^3A state. As can be seen, they are not principally on the Pr atom but have been distributed onto the ligands.

therefore consistent with another resonance below those attributable to the three VOs that are analogous to those in $Yb(tfc)_3$. Of course, it is possible that the normally unoccupied orbitals we show could support a stable negative ion. Our calculations are not sufficiently accurate to determine this quantitative issue. However, the resonances observed in ETS affirm the picture we present.

We have not attempted calculations on $Er(tfc)_3$ and $Eu(tfc)_3$ because they are expected to have much more complicated spin structures. We can, however, make some reasonable conjectures about their structures based upon the number of their f-electrons, the calculated results for $Yb(tfc)_3$ and $Pr(tfc)_3$, and qualitative considerations of ligand field theory. There are seven spatial functions in an f-shell. As mentioned, if these are in a C_3 symmetry environment, first-order perturbations will produce three A and two pairs of E states. The f-orbitals are proportional to $l = 3$ spherical harmonics and the three A-type functions are Y(3,3), Y(3,0), and Y(3,−3) or real linear combinations of them. The sets of E functions are Y(3,±1) and Y(3,±2). Again, real linear combinations of these may be used. Eu^{+3} has six f-electrons. Therefore, no matter how the ligand field causes the occupations among the A or E orbitals to occur, there are not enough electrons to completely fill the E-type orbitals and so there will be E-holes. We expect the $Eu(tfc)_3$ to be in a triplet A state as is $Pr(tfc)_3$. Er^{+3} has eleven f-electrons and this case is not so clear-cut. If the E orbitals were all filled with their maximum of eight electrons, this would leave only three electrons for A orbitals, an unexpected outcome. We suggest a scenario in which there are three holes, one of type A and two of type E. In this case we expect an overall A state, but now with doublet or quartet mulitplicity. We again have the ingredients to produce a low-lying resonance. These results and qualitative considerations imply that $Pr(hfc)_3$, $Eu(hfc)_3$ and $Er(hfc)_3$ may have an extra low-lying resonance compared to $Yb(hfc)_3$.

In summary, as is the case with all filled orbitals, all SOMOs in the neutral ground state of these molecules lie below the vacuum level and thus are not accessible by positive energy electrons. If a SOMO or a filled MO were above the vacuum level, the compound would be unstable with respect to electron

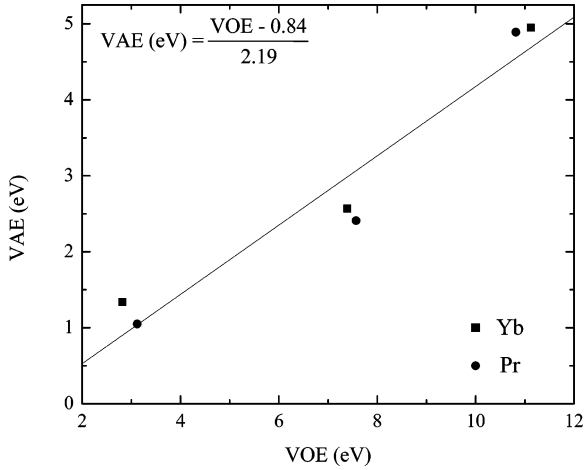

Figure 10. Experimental vertical attachment energies (VAEs) of $Yb(hfc)_3$ and $Pr(hfc)_3$ vs calculated virtual orbital energies (VOEs) of $Yb(tfc)_3$ and $Pr(tfc)_3$. The equation for the line of best fit is shown. The R^2 value is 0.93.

detachment and the stable form of the molecule would exist as a cation. In the case of the heavier $Yb(hfc)_3$, 13 electrons must be accommodated by the three A and two pairs of E sets of orbitals that result from symmetry splitting of the seven original equivalent f-orbitals of the Yb atom. Therefore, no normally unoccupied orbitals are available to produce a very low-energy resonance. In the case of the lighter $Pr(hfc)_3$, only two such electrons occupy the aforementioned set of seven orbitals and with a lesser positive core, it is not surprising that the analogous set of A and E orbitals would be shifted higher in energy. It is thus possible that the unfilled orbitals of the remaining three shift reagents, the analogs of which are all fully or singly occupied in $Yb(hfc)_3$, lie above the vacuum level and may produce a resonance. With $l = 1$, the E-type orbitals are the only ones expected to produce strong scattering.

Results and Discussion

A. Orbital Assignments. We can use the results of these calculations to assign virtual orbitals (VOs) to resonances we observe in the total scattering cross sections. The energy of a VO can be used to approximate the energy of the anion resulting from occupation of that orbital according to Koopmans' theorem.[17] It is well understood that computed energies of VOs are too high because interactions with continuum states are not taken into account.[18] Because the VO energies (VOEs) are near the vacuum level, they are lowered by interaction with continuum states. Another source of error in Koopmans' theorem values is the neglect of electron correlation effects, which also results in a lowering of energy.[19]

In a family of closely related molecules, such as the NMR shift reagents, the correlation between VAEs and VOEs is usually strong. Thus scaling the VOE values can aid in the assignment of specific normally unoccupied orbitals to resonances. Such a procedure was followed recently for molecules consisting of alternating phenyl and ethynyl groups[20] and was done by Modeli[21] for a more general selection of unsaturated hydrocarbons. Figure 10 is a plot of the VAEs of $Yb(hfc)_3$ and $Pr(hfc)_3$ vs the VOEs of $Yb(tfc)_3$ and $Pr(tfc)_3$. The linearity of the VAE/VOE correlation is strong enough that we have confidence assigning the three resonances in $Yb(hfc)_3$ and the upper three resonances in $Pr(hfc)_3$ to the lowest three sets of unoccupied orbitals of type e symmetry shown in Figures 5−7 for $Yb(tfc)_3$. We note that the use of the small "MINI" basis set (required due to the complexity of the molecules) and the

truncation of the saturated C−F chains may lead to greater scatter than would result from an ideal calculation.

B. Electron Circular Dichroism. We now consider our results in the context of the Münster asymmetry measurements.[3,4] Spin-forward and spin-backward longitudinally polarized electrons generally have different scattering cross sections when incident upon chiral molecules. This helicity dependence is called "electron-circular dichroism (ECD)," in analogy with the comparable optical effect involving circularly polarized light. Electron circular dichroism can be characterized by the asymmetry

$$A = \frac{I^+ - I^-}{I^+ + I^-} \tag{1}$$

where $I^{+(-)}$ is the current transmitted through a chiral target of a given handedness, normalized to incident current, for spin forward (backward) electrons. Nonzero values of the asymmetry A have been observed by the Münster group with a variety of targets: bromocamphor, dibromocamphor, (+)-iodomethylbutane, (+)-bromomethylbutane, and the series of NMR shift reagent "propeller molecules" discussed here.[3,4,22] Such collisions provide the chance to study the interesting effects of chiral symmetry on electron-molecule scattering dynamics[23,24] and also hint at the importance of the cosmic-ray background for the origins of biological homochirality.[25] A detailed picture of the electronic molecular structure of chiral targets is crucial to such topics. We have previously detailed the specific mechanisms by which ECD can occur, and refer the reader to refs 6 and 22 for a discussion of chiral collision dynamics.

C. Resonances and ECD. For a given chiral molecule, it is expected that features in the ECD asymmetry A may correspond to resonances in the total electron scattering cross section. A resonance provides greater interaction time between the incident electron and the molecular target, giving the two collision constituents a better chance of "sampling each other's chirality".[23,24] Recently, we studied the correlation between ECD and low-energy electron scattering resonances for bromocamphor and dibromocamphor[6] using ETS. In that paper we showed, with the aid of virtual orbital and helicity density calculations, that resonances observed in ETS between 1 and 7 eV were very likely the sources for certain ECD features. However, other asymmetry structures could not be explained by resonance behavior.

We now use our experimental and theoretical results to comment on this issue for the NMR shift reagents. As can be seen in Figure 11,[4] each of the Münster asymmetry spectra exhibit similar structure, though comparable features are shifted from target to target as indicated with dashed lines. (The local minimum in the (+)-Pr(hfc)$_3$ spectrum at 1.5 eV appears to be caused by the tendency of the observed ECD asymmetries to increase rapidly at low energies due to an experimental artifact.[4]) As can also be seen, there are additional structures at even lower energies (0.75−1.3 eV). These features are clearly visible in all spectra with the exception of Pr(hfc)$_3$. As discussed above, Yb(hfc)$_3$ does not display a low-energy resonance in the total scattering cross section. Thus these ECD structures are almost certainly not related to the lowest energy resonance observed in the other three compounds in ETS. It is probable that similar structures exist in Pr(hfc)$_3$ but are shifted to energies not accessible by the Münster ECD apparatus.

Analyzing the (+)-Yb(hfc)$_3$ ECD spectrum (black dots) above 2 eV, one observes a strong peak at approximately 2.5 eV, followed by a shoulder near 4 eV, then a minimum near 5.6 eV. Analogous features in (+)-Pr(hfc)$_3$ occur at lower energies, namely 1.9, ∼3 and 4.7 eV. We suggest that analogous features appearing in the spectrum of each compound are caused by the same dynamical scattering mechanism. *Thus the resonance bands shown in Figure 2 of ref 4, which are very similar in energy across the molecular family, are not always centered on the ECD feature for which the indicated resonance may be responsible.* In the case of Yb(hfc)$_3$, ref 3 provides evidence that the three major resonances observed by the Münster group in ETS (Figure 4 of ref 3) are responsible for three specific prominent features in the ECD data. Their resonance energies correlate closely with pronounced ECD minima at 1.5 and 5.6 eV and a maximum at 2.5 eV. The same is seen for Er(hfc)$_3$.[4] Based on these two cases and the similarity of the Yb(hfc)$_3$ ET spectra of this work to that given in ref 3, the assignment of these three asymmetry features to the orbitals shown in Figures 5−7 is reasonable. However, one would expect the analogous ECD features in the Eu(hfc)$_3$ and Pr(hfc)$_3$ to correlate with the parallel resonances. Yet the ECD features in these two compounds are shifted to significantly lower energies with only a slight shift in the VAEs (see Table 1 and Figure 2 of ref 4).

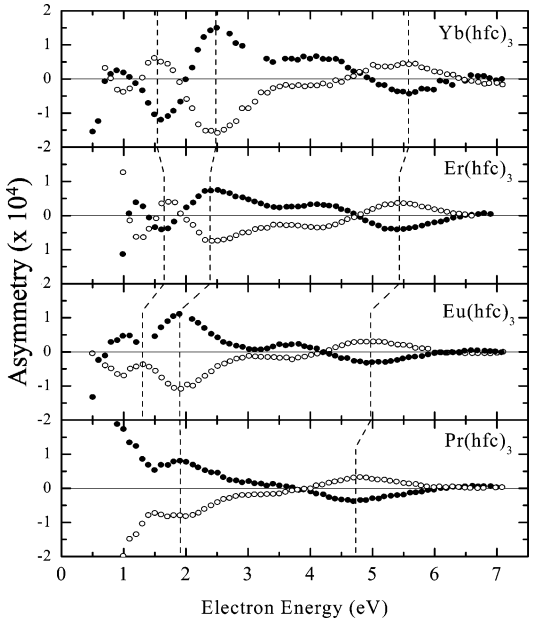

Figure 11. Asymmetry vs incident electron energy of the NMR shift reagents reproduced from ref 4. The data points for the + enantiomers are shown as black dots and open circles are the data points for the − enantiomers. Error bars are not shown but are generally comparable to or smaller than the size of the data points above 2.0 eV. They increase to $\sim 2 \times 10^{-5}$ below 2.0 eV.

The ligands in the Münster experiment[4] were of pure chirality (either all right-handed or all left-handed), but their arrangement about the central high-*Z* atom was racemic. Thus the target's "integrated" stereochemical chirality existed not on the high-*Z* target center, but on each of the individual ligands. Figures 5 and 6 show that the orbitals responsible for the two lowest energy ETS resonances in Yb(hfc)$_3$ and the two middle resonances in the remaining compounds are predominately located on the six-membered ring structures discussed earlier that join the central atom with the ligands. Little wave function amplitude exists on chiral centers of the ligands. In the "resonance" model of ECD, this would indicate that the extra electron involved in these TNIs would not be expected to exhibit strongly dichroic scattering. Figure 7 shows that the orbitals associated with the broad, high-energy resonances have significant amplitude on the ligand's chiral centers away from the

molecular centers. However, the width of these resonances (>3 eV) is such that ascertaining their involvement in ECD is speculative. It is interesting to note that generally comparable ECD features are shifted lower in energy as the atomic number of the central atom decreases, indicating the global importance of this parameter, outside the context of resonances, to the dynamics of ECD.[6,23] When this is considered along with the fact that (a) shifts in resonance energies do not correlate with energy trends seen in the ECD asymmetries and that (b) the wave functions of the relevant orbitals do not have significant overlap with the targets' chiral centers, we conclude that resonance behavior is not or is only partly responsible for the ECD structures.

Conclusions

The chemistry involving temporary negative ions of large molecules plays principal roles in many important systems ranging from biological molecules[26] to the remediation of pesticides.[27] Understanding the orbitals associated with TNI formation is central to deducing mechanistic information of these processes. In this study we have demonstrated that reliable orbital assignments are possible for molecules with large (>1200) atomic weights. With electron transmission spectroscopy measurements and ROHF calculations on a sereies of NMR shift reagents, we have assigned resonances in the total cross sections to normally unoccupied orbitals. In contrast to our previous study of bromocamphor and dibromocamphor,[6] only tenuous evidence is seen for resonance involvement in ECD exhibited by the NMR shift reagents. The proximity of VAEs to strong features in the ECD spectra for the Yb and Er targets seemingly provides strong evidence for resonance behavior in the production of ECD. However, our analysis, aided by our new ETS measurements and computational results, demonstrate that significant shifts in analogous ECD features across the NMR shift reagents are not met with similar changes in VAEs, as would be expected if the two phenomena were clearly connected. The correlation in these ECD features with the *Z* value of the central lanthanide atom may indicate the involvement of a consistent dynamical scattering mechanism. The complexity of the NMR shift reagent molecules makes it difficult to ascertain a particular mechanism at this time, and further inquiry into this subject would be worthwhile.

Acknowledgment. We thank Dr. Paul D. Burrow for the use of the electron transmission spectrometer and Dr. Kayvan Aflatooni for preliminary work involving the $Yb(hfc)_3$ compound. This work was funded by NSF Grant PHY-0653379.

References and Notes

(1) See, for example: Barrios, R.; Skurski, P.; Simons, J. *J. Phys. Chem. B* **2002**, *106*, 7991.
(2) Sanche, L.; Schulz, G. J. *Phys. Rev. A* **1972**, *5*, 1672.
(3) Mayer, S.; Nolting, C.; Kessler, J. *J. Phys. B* **1996**, *29*, 3497.
(4) Nolting, C.; Mayer, S.; Kessler, J. *J. Phys. B* **1997**, *30*, 5491.
(5) Aflatooni, K.; Gallup, G. A.; Burrow, P. D. *J. Phys. Chem. A* **2000**, *104*, 7359.
(6) Scheer, A. M.; Gallup, G. A.; Gay, T. J. *J. Phys. B* **2006**, *39*, 2169.
(7) Stamatovic, A.; Schulz, G. J. *Rev. Sci. Instrum.* **1970**, *41*, 423.
(8) Johnston, A. R.; Burrow, P. D. *J. Electron Spectrosc. Relat. Phenom.* **1982**, *52*, 119.
(9) Jorgensen, C. K. *Modern Aspects of Ligand Field Theory*; American Elsevier: Amsterdam, 1971.
(10) Schmidt, M. W.; Baldridge, K. K.; Boatz, J. A.; Elbert, S. T.; Gordon, M. S.; Jensen, J. H.; Koseki, S.; Matsunaga, N.; Nguyen, K. A.; Su, S. J.; Windus, T. L.; Dupuis, M.; Montgomery, J. A. *J. Comput. Chem.* **1993**, *14*, 1347.
(11) Huzinaga, S.; Andzelm, J.; Klobukowski, M.; Radzio-Andzelm, E.; Sakai, Y.; Tatewaki, H *Gaussian Basis Sets for Molecular Calculations*; Elsevier: Amsterdam, 1984.
(12) Gallup, G. A.; Vance, R. L.; Collins, J. R.; Norbeck. J. M. *Adv. Quantum Chem.* **1982**, *16*, 229.
(13) Gallup, G. A. *Valence Bond Methods*; Cambridge University Press: Cambridge, 2002.
(14) Portmann, S. *Chimia* **2000**, *54*, 766. See Molekel http://www.csc-s.ch/molekel/.
(15) Gallup, G. A. *J. Chem. Phys.* **1966**, *45*, 2304.
(16) Burrow, P. D.; Jordan, K. D. *Chem. Rev.* **1987**, *87*, 557.
(17) Koopmans, T. *Physica* **1933**, *1*, 105.
(18) Chen, D.; Gallup, G. A. *J. Chem. Phys.* **1990**, *93*, 12.
(19) Staley, S. W.; Strnad, J. T. *J. Phys. Chem.* **1994**, *98*, 116.
(20) Scheer, A. M.; Burrow, P. D. *J. Phys. Chem. B* **2006**, *110*, 17751.
(21) Modelli, A. *Phys. Chem. Chem. Phys.* **2003**, *5*, 2923.
(22) Mayer, S.; Kessler, J. *Phys. Rev. Lett.* **1995**, *74*, 4803.
(23) Gay, T. J.; Johnston, M. E.; Trantham, K. W.; Gallup, G. A. In *Selected Topics in Electron Physics*; Campbell, D. M., Kleinpoppen, H., Eds.; Plenum: New York, 1996.
(24) Stephen, T. M.; Shi, X.; Burrow, P. D. *J. Phys. B* **1988**, *21*, 169.
(25) Keszthelyi, L. *Q. Rev. Biophys.* **1995**, *28*, 473.
(26) See, for example, Scheer, A. M.; Aflatooni, K.; Gallup, G. A.; Burrow, P. D. *Phys. Rev. Lett.* **2004**, *93*, 068102.
(27) Burrow, P. D.; Aflatooni, K.; Gallup, G. A. *Environ. Sci. Technol.* **2000**, *34*, 3368.